Robust estimations of the region of attraction using invariant sets

Andrea Iannelli[a,*], Andrés Marcos[a], Mark Lowenberg[a]

[a] *Department of Aerospace Engineering, University of Bristol, BS8 1TR, United Kingdom*

Abstract

The Region of Attraction of an equilibrium point is the set of initial conditions whose trajectories converge to it asymptotically. This article, building on a recent work on positively invariant sets, deals with inner estimates of the ROA of polynomial nonlinear dynamics. The problem is solved numerically by means of Sum Of Squares relaxations, which allow set containment conditions to be enforced. Numerical issues related to the ensuing optimization are discussed and strategies to tackle them are proposed. These range from the adoption of different iterative methods to the reduction of the polynomial variables involved in the optimization. The main contribution of the work is an algorithm to perform the ROA calculation for systems subject to modeling uncertainties, and its applicability is showcased with two case studies of increasing complexity. Results, for both nominal and uncertain systems, are compared with a standard algorithm from the literature based on Lyapunov function level sets. They confirm the advantages in adopting the invariant sets approach, and show that as the size of the system and the number of uncertainty increase, the proposed heuristics ameliorate the commented numerical issues. [1]

Keywords: Region of attraction, Robust analysis, Nonlinear dynamics, Sum of squares, Uncertainties, Local analysis

1. Introduction

In the analysis of nonlinear systems, it is of paramount importance the concept of asymptotic stability of an equilibrium point x^* (in the sense of Lyapunov). If fulfilled, this property guarantees the existence of a *neighbourhood* of x^* such that all the states trajectories starting in it eventually converge to the equilibrium. Global asymptotic stability ensures that this is true for any trajectory, no matter how far from x^* it starts. However, an inherently nonlinear

*Corresponding author

Email address: andrea.iannelli@bristol.ac.uk (Andrea Iannelli)

[1] A MATLAB-implementation of the algorithms developed in the paper is available at the following link: https://github.com/AndreaIan/ROA-invariant-robust

feature is that this can hold only locally, and therefore the notion of Region of Attraction (ROA) has been proposed. The ROA of an equilibrium point is the set of all the initial conditions from which the trajectories of the system converge to x^* as time goes to infinity [1], and its knowledge is of practical interest to guarantee the safe operation of nonlinear systems.

Finding analytically the exact region of attraction might be difficult or, depending on the complexity of the system, even impossible [2]. Several algorithms have thus been proposed to numerically calculate inner Estimates of the Region of Attraction (ERA), which can be broadly classified into two categories: Lyapunov methods and non-Lyapunov methods.
The former build on the invariance and contractiveness properties held by Lyapunov functions (LF) sublevel sets. When the LF space is restricted to quadratic functions, an ERA for polynomial (or even rational) systems is the largest ellipsoid obtained by computing the Lyapunov matrix [3], whose calculation can be posed as a line search involving the solution of a series of Linear Matrix Inequalities (LMIs). In the general case of higher order LF, Sum Of Squares (SOS) techniques can be used to recast the problem as a set of SemiDefinite Programs (SDPs) [4]. For example, in [5] an algorithm, named V-s iteration, is formalised to solve the (non-convex) Bilinear Matrix Inequalities (BMI) needed for evaluating LFs of arbitrary degree, whereas in [6] a BMI solver is directly employed to determine composite LF level sets.
Non-Lyapunov methods have also been studied to reduce the conservatism typically associated with the aforementioned approaches. In [7] it is shown that the problem can be formulated as a convex infinite-dimensional linear program, which is solved by making use of the concept of occupation measures. The use of Integral Quadratic Constraints to provide ROA certificates for systems subject to generic nonlinearities was recently proposed in [8], whereas in [9, 10] the recipes for calculating ERA are expressed in terms of positively invariant sets. The latter approaches, prompted by the LaSalle's theorem [1], still use Lyapunov stability concepts but relax the conditions that must be fulfilled by the function used to define the ERA.

This article considers the algorithm from [9] as starting point. The first objective is to provide a comparison of results using approaches belonging to the Lyapunov methods class. Based on two case studies from the literature featuring increasing complexity, the goal is to verify and quantify the reduction in conservatism obtained by the invariant sets approach. The second contribution is to propose an algorithm, within the context of positively invariant sets, to determine robust inner Estimates of the Region of Attraction (rERA), i.e. ERA of systems with uncertain parameters. This problem was not the focus in [9] and thus was only marginally considered therein, but has been studied by other researchers in the past.

Within the Lyapunov method class of approaches, a first important distinction concerns the dependence of the sought LF on the uncertain parameters. In [11] an algorithm restricted to systems with a specific dependence on the uncertainties (e.g. uncertain parameters appearing affinely) is proposed, based on parameter-independent LF, i.e. a single Lyapunov function is used to

certify the local stability of a system over the entire parameters space. This was refined in [12] allowing for a branch-and-bound improvement to alleviate the conservatism associated with the parameter-independent LF. Other studies considered parameter-dependent LFs [13, 6], with the ensuing SOS-based optimization problem featuring a substantial increase in computational burden. Recent works [14, 15] addressed this problem by computing rational Lyapunov functions of the states and uncertain parameters without recurring to SOS relaxations. In [14] Finsler's Lemma and the notion of annihilators are employed to formulate affine parameter dependent LMIs conditions for systems with rational vector fields. A further improvement of this algorithm is proposed in [15] where a method based on Linear Fractional Transformations is developed, which allows for a more efficient computation of the LF by informing the selection of the rational terms. Drawbacks of these approaches are the conservativeness associated with the adoption of LF level sets and the dependence of the level sets on the uncertain parameters, which makes more difficult the interpretation of the results. In view of these well recognised and conflicting aspects, in Section 5 a numerical method to study robust ROA by means of invariant sets is proposed. The main feature is that the rERA is expressed via a parameter-independent level set, with the discussed advantages, but conservatism is reduced by introducing in the formulation a second function which is allowed to depend on the uncertainties.

Finally, it is worth remarking that the usage of SOS techniques often leads to bilinear problems [16], and iteration schemes are employed. This topic has not received large attention in the community, therefore various numerical strategies to efficiently solve the resulting non-convex optimization problems and mitigate numerical issues typically arising when using SOS are investigated and commented in Section 3.

The article, which builds on preliminary results presented in [17, 18], is structured as follows. Section 2 establishes the notation and required fundamental definitions. Section 3 presents the problem of determining estimates of the ROA for nominal systems and describes iterative schemes which are subsequently applied in Section 4. Section 5 finally deals with estimations of the robust region of attraction, and Section 6 presents the Conclusions and future evolutions of the work.

2. Notation and definitions

The set of functions $g(x) : \mathbb{R}^n \to \mathbb{R}$ which are m-times continuously differentiable is denoted by $\mathcal{C}^m$. For $x \in \mathbb{R}^n$, the set of all polynomials in n variables is denoted by $\mathbb{R}[x]$. For $g \in \mathbb{R}[x]$, $\partial(g)$ denotes the degree of g. Given a scalar $c > 0$, the level set of g and its boundary are defined as:

$$\begin{aligned} \varepsilon(g, c) &:= \{x \in \mathbb{R}^n : g(x) \leq c\}, \\ \partial\varepsilon(g, c) &:= \{x \in \mathbb{R}^n : g(x) = c\}. \end{aligned} \tag{1}$$

A polynomial $g(x)$ is said to be a sum of squares if there exists a finite set of polynomials $g_1(x), ..., g_k(x)$ such that $g(x) = \sum_{i=1}^{k} g_i^2(x)$. The set of SOS

polynomials in x is denoted by $\Sigma[x]$. The importance of SOS polynomials is due to their connection with convex optimization [19]. A given polynomial $g(x)$ with $\partial(g) = 2d$ can be expressed as a quadratic form in all the monomials of degree less than or equal to d, i.e. $g = z^T Q z$ where $z = [1, x_1, x_2, ..., x_n, x_1 x_2, ..., x_n^d]$. Since the variables in z are not algebraically independent, the matrix Q is not unique. In fact, it can be shown that the set of matrices Q satisfying the previous relation is an affine subspace. Most importantly, $g \in \Sigma[x]$ if and only if $Q = Q^T \succeq 0$, that is Q, named the Gram matrix, is positive semidefinite. This problem can be tackled by solving a semidefinite program (SDP) [20] and there are freely available software toolboxes allowing to accomplish this in an efficient manner. In this work, the software SOSOPT from the suite of libraries [21] will be used in conjunction with the SDP solver Sedumi [22]. As for the computational aspects, note that if g is dense (i.e. no sparse monomials), the dimension of the Gram matrix is $\binom{n+d}{d}$. This means that the size of the SDP problem N_{SDP} grows polynomially with n if d is fixed (and vice versa), but it grows exponentially if both n and d increase.

Consider an autonomous nonlinear system of the form

$$\dot{x} = f(x), \quad x(0) = x_0, \tag{2}$$

where $f : \mathbb{R}^n \to \mathbb{R}^n$ is the vector field. The vector $x^* \in \mathbb{R}^n$ is called a *fixed* or *equilibrium* point of (2) if $f(x^*) = 0$. Let us denote by $\phi(t, x_0)$ the solution of (2) at time t with initial condition x_0. Then, the Region of Attraction associated with x^* is defined as:

$$\mathcal{R} := \left\{ x_0 \in \mathbb{R}^n : \lim_{t \to \infty} \phi(t, x_0) = x^* \right\}. \tag{3}$$

That is, $\mathcal{R}$ is the set of all initial states that eventually converge to x^*. While for linear systems convergence to the equilibrium is a global property, for nonlinear ones it might hold only locally (i.e. $\mathcal{R} \subseteq \mathbb{R}^n$). The origin will be assumed as fixed point ($x^* = 0$) henceforward without loss of generality.

3. Computation of nominal ERAs using invariant sets

The paper focuses on inner Estimates of the Region of Attraction formulated as compact positively invariant sets and computed by means of Sum Of Squares techniques. This section presents the main theoretical result from [9] and discusses numerical algorithms to find the ERA under the assumption of nominal vector field (2). A novel algorithm is proposed (Subsection 3.2) that ameliorates the computational effort and improves the level sets estimates. This is also used to devise a hybrid algorithm (Subsection 3.3) aimed to tackle some of the pitfalls associated with SOS optimization.

3.1. From Lyapunov functions to positively invariant level sets

A standard approach to calculate ERA consists in applying the Lyapunov's direct method as defined next.

Lemma 1. *[1] Let $\mathcal{D} \subset \mathbb{R}^n$ and let $x^*(=0)$ be contained in $\mathcal{D}$. If there exists $V : \mathbb{R}^n \to \mathbb{R}$, with $V \in \mathcal{C}^1$ such that*

$$\begin{aligned} &V(0) = 0 \quad \text{and} \quad V(x) > 0 \quad \forall x \in \mathcal{D}\backslash 0, \\ &\dot{V}(x) = \nabla V(x) f(x) < 0 \qquad \forall x \in \mathcal{D}\backslash 0, \\ &\varepsilon(V, c) \quad \text{is bounded and} \quad \varepsilon(V, c) \subseteq \mathcal{D}, \end{aligned} \tag{4}$$

then $\varepsilon(V, c)$ is an invariant set of $\mathcal{R}$.

LeSalle's theorem [1] points out that this characterization is usually conservative due to the fact that contractiveness of the level set defining the ERA is unnecessary. In fact, it suffices to consider compact positively invariant subsets of $\mathcal{D}$, that is, a compact set $\Omega \subseteq \mathcal{D}$ such that every trajectory starting in Ω stays in Ω for all future time. Invariance of Ω typically requires conditions on its boundary to ensure that trajectories starting inside cannot leave.
Prompted by these observations, the following result has been proposed in the literature:

Theorem 1. *([9], Th. 1) If there exist $R, V_N : \mathbb{R}^n \to \mathbb{R}$, with $R, V_N \in \mathcal{C}^1$, and a positive scalar γ satisfying:*

$$\nabla R(x) f(x) < 0 \qquad \forall x \in \partial\varepsilon(R, \gamma), \tag{5a}$$

$$V_N(0) = 0 \quad \text{and} \quad V_N(x) > 0 \quad \forall x \in \varepsilon(R, \gamma)\backslash 0, \tag{5b}$$

$$\nabla V_N(x) f(x) < 0 \qquad \forall x \in \varepsilon(R, \gamma)\backslash 0, \tag{5c}$$

$$\varepsilon(R, \gamma) \quad \text{is compact and} \quad 0 \in \varepsilon(R, \gamma), \tag{5d}$$

then $\varepsilon(R, \gamma)$ is an invariant set of $\mathcal{R}$.

The proof of this result can be found in [9]. The fundamental idea is that $\varepsilon(R, \gamma)$ is a positively invariant set, due to (5a)-(5d), and that all trajectories initiated from it converge to a level set of some LF, which is contractive and invariant because of (5b)-(5c), therefore guaranteeing such set to be an ERA. Note that the level set defined by R is not contractive, in that only negativity of the gradient ∇R on the set boundary is required.

Theorem 1 involves finding functions that satisfy set containment conditions. In order to make the problem computationally tractable, attention is restricted to polynomial vector fields f. Known results from real algebraic geometry, which focuses on the relationship between geometric objects and the associated abstract algebraic structures, can then be employed to tackle this problem. In particular, an application of the Positivstellensatz (P-satz) Theorem [23] allows the following property to be stated.

Lemma 2. *[19] Given $h, f_0, ..., f_r \in \mathbb{R}[x]$, the following set containment holds*

$$\big\{x : h(x) = 0, f_1(x) \geq 0, ..., f_r(x) \geq 0\big\} \subseteq \big\{x : f_0(x) \geq 0\big\}, \tag{6}$$

if there exist multipliers *$p \in \mathbb{R}[x]$, $s_{01}, ..., s_{0r} \in \Sigma[x]$ such that*

$$p(x)h(x) - \sum_{i=1}^{r} s_{0i}(x) f_i(x) + f_0(x) \in \Sigma[x]. \tag{7}$$

This result generalizes the well known S-procedure [20], which applies to quadratic functions, to the case of generic degree and allows the set containments in Lemma 1 to be expressed as SOS constraints. The ERA formulated in Th. 1 can indeed be certified with the following lemma:

Lemma 3. *[9] Let V_N and R be multivariable polynomials and γ a positive scalar. If there exist SOS polynomials s_1, s_2 and a polynomial s_0 such that:*

$$
\begin{aligned}
-\nabla R f - s_0(\gamma - R) &\in \Sigma[x], && \text{(8a)}\\
V_N - s_1(\gamma - R) &\in \Sigma[x], && \text{(8b)}\\
-\nabla V_N f - s_2(\gamma - R) &\in \Sigma[x], && \text{(8c)}
\end{aligned}
$$

then the inequalities (5) are satisfied and $\varepsilon(R,\gamma)$ is an ERA of the origin.

The following SOS program can be employed to enlarge the provable ERA based on Lemma 3.

Program 1.

$$
\begin{aligned}
&\max_{s_1,s_2\in\Sigma[x];\ \ s_0,V_N,R\in\mathbb{R}[x]} \gamma\\
&\text{subject to conditions (8a-8b-8c).}
\end{aligned}
\qquad (9)
$$

It is important to observe that V_N and R are now part of the optimization. While the former enters affinely in (9), there are bilinear terms featuring the multipliers s_i, γ and R. If one of the two terms in the bilinearity (e.g. $s_0\gamma$) is the objective function, it was demonstrated that the problem is quasiconvex [24], hence the global optimum can be computed via cost bisection. However the terms in s_i and R (e.g. $s_0 R$) makes the above program non-convex. This can be handled with local BMI solvers [25] or by means of iterative schemes. In [9] the latter approach is adopted and the following 2-steps algorithm is proposed.

Algorithm 1. *(IS - 2 Steps)*
Output: *the level set $\varepsilon(R,\gamma)$ (inner estimate of the ROA).*
Input: *a polynomial R^0 satisfying (8a) for some γ.*

Step A1-1 : optimize V_N and multipliers through bisection on γ

$$
\begin{aligned}
&\max_{s_1,s_2\in\Sigma[x];s_0,V_N\in\mathbb{R}[x]} \gamma\\
&-\nabla R^0 f - s_0(\gamma - R^0) \in \Sigma[x]\\
&V_N - s_1(\gamma - R^0) \in \Sigma[x]\\
&-\nabla V_N f - s_2(\gamma - R^0) \in \Sigma[x]
\end{aligned}
$$

set $\bar\gamma \leftarrow \gamma, \bar s_\# \leftarrow s_\#, \# = 0,1,2$

Step A1-2 : optimize V_N and R through bisection on γ

$$
\begin{aligned}
&\max_{s_3\in\Sigma[x];V_N,R\in\mathbb{R}[x]} \gamma\\
&-\nabla R f - \bar s_0(\gamma - R) \in \Sigma[x]\\
&V_N - \bar s_1(\gamma - R) \in \Sigma[x]\\
&-\nabla V_N f - \bar s_2(\gamma - R) \in \Sigma[x]\\
&(\gamma - R) - s_3(\gamma - R^0) \in \Sigma[x]\\
&\gamma - \bar\gamma \geq 0
\end{aligned}
$$

set $R^0 \leftarrow R$ and go to Step A1-1

This iterative scheme consists of two steps. In Step 1 the multipliers $s_{\#}$ and V_N are optimised, whereas Step 2 computes again V_N and the level set function R, which is updated at the beginning of the new iteration ($R^0 \leftarrow R$). The iterations terminate when one of the steps fails, i.e. the associated optimization is found unfeasible, and the last optimised values for R and γ are taken to provide the output $\varepsilon(R, \gamma)$. This approach is adopted for all the algorithms discussed in the paper. Alternatively, a stopping criterion could be employed to prevent slow progress in the simulations. This is not done here in order to present an objective comparison among the algorithms, free from arbitrariness as for example the choice for the tolerance on the progress. The last two constraints in Step 2 ensure that $\varepsilon(R^0, \gamma) \subseteq \varepsilon(R, \gamma)$, i.e. the solution is a set that strictly contains the previous one.
Note that a candidate R is required to initialise the algorithm. A possible choice is any quadratic LF proving asymptotic stability of the linearised system (provided that the associated Jacobian is Hurwitz), denoted V_{lin}.

3.2. A 3 step iteration scheme

An alternative algorithm to solve Program 1 is proposed here. The aim is on the one hand to improve the run time, and on the other to overcome issues typically arising when employing SOS (e.g. infeasibility of the program for numerical reasons). First, a modification of Algorithm 1 is discussed. The last two constraints in Step A1-2 commented before make Step A1-2, in addition to Step A1-1, quasi-convex. To make it convex, the last two SOS constraints in Step A1-2 are replaced with:

$$(\gamma - R) - s_3(\bar{\gamma} - R^0) \in \Sigma[x]. \tag{10}$$

By direct application of Lemma 2, this constraint enforces $\varepsilon(R^0, \bar{\gamma}) \subseteq \varepsilon(R, \gamma)$. Thus, the estimated ROA increases at each iteration, but this is achieved now without introducing bilinearities. In the tested cases this modification led to a reduction in simulation and better accuracy in the results. Therefore, this is implemented in all the analyses shown here (i.e. Algorithm 1 represents already an improvement compared to the baseline proposed in [9]).

In addition to this, a new iteration strategy is devised which consists of splitting Step A1-1 into two steps, Step A2-1 and Step A2-2. This aims at easing the numerical solution of Program 1 by using first an initial guess V_N^0 to find the required multipliers s_0, s_1, s_2 in Step A2-1, and then computing the optimal V_N in Step A2-2. Step A2-3 embeds the aforementioned modification proposed for Step A1-2. This 3 steps iteration scheme is reported in the following.

Algorithm 2. *(IS - 3 Steps)*
Output: *the level set $\varepsilon(R,\gamma)$ (inner estimate of the ROA).*
Input: *polynomials R^0, V_N^0 satisfying (8) for some γ.*

Step A2-1 : optimize the multipliers for fixed level sets shapes

$$\max_{s_1,s_2\in\Sigma[x];s_0\in\mathbb{R}[x]} \gamma$$
$$-\nabla R^0 f - s_0(\gamma - R^0) \in \Sigma[x]$$
$$V_N^0 - s_1(\gamma - R^0) \in \Sigma[x]$$
$$-\nabla V_N^0 f - s_2(\gamma - R^0) \in \Sigma[x]$$

set $\bar{\gamma} \leftarrow \gamma, \bar{s}_\# \leftarrow s_\#, \# = 0,1,2$

Step A2-2 : optimize V_N

$$\max_{V_N\in\mathbb{R}[x]} \gamma$$
$$-\nabla R^0 f - \bar{s}_0(\gamma - R^0) \in \Sigma[x]$$
$$V_N - \bar{s}_1(\gamma - R^0) \in \Sigma[x]$$
$$-\nabla V_N f - \bar{s}_2(\gamma - R^0) \in \Sigma[x]$$
$$\gamma \geq \bar{\gamma}$$

set $\bar{V}_N \leftarrow V_N, \bar{\gamma} \leftarrow \gamma$

Step A2-3 : optimize R

$$\max_{s_3\in\Sigma[x];R\in\mathbb{R}[x]} \gamma$$
$$-\nabla R f - \bar{s}_0(\gamma - R) \in \Sigma[x]$$
$$\bar{V}_N - \bar{s}_1(\gamma - R) \in \Sigma[x]$$
$$-\nabla \bar{V}_N f - \bar{s}_2(\gamma - R) \in \Sigma[x]$$
$$(\gamma - R) - s_3(\bar{\gamma} - R^0) \in \Sigma[x]$$

set $R^0 \leftarrow R, V_N^0 \leftarrow \bar{V}_N$ and go to Step A2-1

The scheme consists of one quasi-convex step (Step A2-1) and two convex steps (Step A2-2 and Step A2-3). Each step has a specific task: Step A2-1 provides the multipliers for the next two steps; Step A2-2 calculates the function V_N; and Step A2-3 evaluates the sought level set $\varepsilon(R,\gamma)$ based on the iterates from the previous steps. The size γ of the ERA is maximised throughout each iteration, although Steps Step A2-2 and Step A2-3 can also be solved as simple feasibility problems. In this regard, note that the optimality of the solution is already prevented by the non-convexity of (9), and that the algorithm ensures in any case that the ERA is non-decreasing. Therefore, resorting to just feasibility when maximization fails is a viable solution.

Algorithm 2 requires initializations for R and V_N. A first option is to choose for both V_{lin}, which automatically satisfies (8) for sufficiently small γ. Alternatively, the calculation can start with Algorithm 1 which in turn can provide the initializations R^0 and V_N^0 to Algorithm 2. It is stressed the importance of the fact that Algorithm 2 is initialized with both the functions R and V_N. This feature can be favourably used when preliminary estimations of the *shape* of the ERA are available in that the search can be seeded with them. In fact, while in

Algorithm 1 this information would be partially lost because the function V_N is optimised anew with the multipliers in Step A1-1, Algorithm 2 optimizes first the multipliers based on the provided estimations of R and V_N, and then adjusts V_N and R correspondingly in the next two steps. Even though the problem remains non-convex (and thus it cannot be guaranteed that the global optimum is found), the formulation of this iterative scheme privileges *local* searches, therefore can represent an important complement to Algorithm 1. This observation represents the premise for the hybrid algorithm described in the next section and leveraging the different features of the two algorithms presented so far.

Finally, the sensitivity of the estimations to the initial guess is in general an important aspect when dealing with SOS-based computations of the ROA [9]. Despite the impossibility to give conclusive statements, Section 4 will investigate this effect (when not specified, the algorithms are initialised with V_{lin}).

3.3. Hybrid scheme

The issues typically arising when computing ERA with SOS-based techniques are twofold: the non-convexity due to the bilinear terms forces coordinate-wise search algorithms to be adopted, inevitably leading to local optima; the SDP associated with each iteration can be computationally challenging, both in terms of run time and accuracy. In an attempt to ameliorate the latter behaviour, in Section 3.2 Algorithm 2 was proposed, which is nonetheless affected by the same local optima pitfall.

The issue of local optima is well-known in the optimization field and one of the proposed solutions is represented by so-called hybrid strategies [26]. The essence of this approach is to cross global optimizers with problem-specific local search algorithms. In the currently investigated programs, the non-convexity is inherent to the adoption of SOS relaxations for the enforcement of set containments. Thus, hybrid schemes meant in the conventional sense do not look viable. However, in this work the availability of the two distinct Algorithms 1 and 2 is exploited to implement a unified iteration scheme which makes the search of ERA more robust to numerical issues. Taking the cue from this discussion, the following *hybrid* algorithm is proposed.

Algorithm 3. *(IS - Hyb)*
Output: *the level set $\varepsilon(R,\gamma)$ (inner estimate of the ROA).*
Input: *a switching criterion sw_{cr}; polynomials R^0, V_N^0 satisfying (8) for some γ.*

Stage 1 :Execute Algorithm 1

if Stage 1 converged **then** set $R^0 \leftarrow R$ and $V_N^0 \leftarrow V_N$

if sw_{cr} is true **then** go to Stage 2

else restart Stage 1

else go to Stage 2

Stage 2 :Execute Algorithm 2

if Stage 2 converged **then** set $R^0 \leftarrow R$ and $V_N^0 \leftarrow V_N$

if sw_{cr} is true **then** go to Stage 1

else restart Stage 2

else set go to Stage 1

The iterative scheme builds on the advantageous capability of switching from one algorithm to the other in case of failed solution or slow progress. The switching criterion sw_{cr} can be formulated based on the idea of associating with each Stage a *reward* [27], that is, a figure of merit of the executed algorithm. If performance in terms of slow progress is considered, the size of the level set γ can be employed. A possible metric to quantify the expansion rate of the ERA for a certain algorithm is obtained comparing values of γ referred to the *same* shape function R. The cost bisections in the first steps of both the algorithms (Step A1-1 and Step A2-1) are performed keeping fixed R at the value of the previous iteration. Thus, sw_{cr} can be defined as a tolerance on the ratio between γ computed at the end of the first step and at the end of the previous iteration respectively. Note that when Algorithm 2 is employed, another choice for sw_{cr} is the ratio between γ computed at Step A2-2 and Step A2-1 respectively, because the shape R is held fixed over the two steps. The number of failures in convergence experienced by the used algorithm can also be used to define the reward, because it reveals the suitability of adopting a certain search strategy for the problem considered.

The adoption of a switching criterion can reduce the run time by pointing at *faster* search directions, and can help taking advantage of the different features of the two algorithms. However, it should not be underestimated the utility of a scheme whose goal is simply to carry on the optimization in case of failed solution of one algorithm. It is indeed often the case that infeasibility of one of the steps is not caused by the fact that the ERA is close to the actual ROA (and thus that no further optimization is possible), but by numerical issues of the SDPs (exacerbated when the size of the program increases). This aspect motivates the choice made in this work of testing Algorithm 3 with sw_{cr} defined such that the algorithm crosses the Stages sequentially (i.e. the inner **if** condition is always true). The selection of sw_{cr} is deemed a problem-specific feature, and the study of alternative solutions is on itself an interesting research study that

can be undertaken in future works focused on the study of ROA with hybrid approaches.

3.4. V-s iteration

This section concludes presenting another algorithm known as $V-s$ iteration (from reference [5]). This algorithm allows to solve the ROA problem using the LF level set approach, and is given as it will serve in the next section as a benchmark to the invariant set original algorithm (IS - 2 Steps) and the newly proposed ones (IS - 3 Steps and IS - Hyb).

Lemma 1 is the starting point, and the resulting set containment conditions are transformed into SOS constraints similarly to what was done previously.

Algorithm 4. *(LF)*
Output: *the level sets $\varepsilon(V,\gamma)$ and $\varepsilon(p,\beta)$ (both inner estimates of the ROA).*
Input: *a polynomial V^0 satisfying (4) for some γ.*

γ***-Step*** : bisect on γ
for a given V
$\max_{s_1 \in \Sigma[x]} \gamma$
$-\nabla V^0 f - s_1(\gamma - V_0) \in \Sigma[x]$

set $\bar{\gamma} \leftarrow \gamma, \bar{s}_1 \leftarrow s_1$

β***-Step*** : maximize the size of
$\varepsilon(p,\beta)$ such that $\varepsilon(p,\beta) \subseteq \varepsilon(V,\gamma)$
$\max_{s_2 \in \Sigma[x]} \beta$
$(\bar{\gamma} - V^0) - s_2(\beta - p) \in \Sigma[x]$

set $\bar{\beta} \leftarrow \beta, \bar{s}_2 \leftarrow s_2$

V-Step : compute a new shape V for a given γ
$V \in \Sigma[x]$;
$-\nabla V f - \bar{s}_1(\bar{\gamma} - V) \in \Sigma[x]$
$(\bar{\gamma} - V) - \bar{s}_2(\bar{\beta} - p) \in \Sigma[x]$

set $V^0 \leftarrow V$ and go to γ-Step

An important difference compared to Algorithm 1, other than the obvious one relative to the problem solved, is the usage of a *given* shape function p. Given $N \in \mathbb{R}^{n\times n}$, $N = N^T > 0$ (shape matrix), the shape function $p(x) = x^T N x$ defines an ellipsoid based on important directions in the state space. The goal of the optimization is to maximize the value of β for which the containment of $\varepsilon(p,\beta)$ in $\varepsilon(V,\gamma)$ can be certified. $\varepsilon(V,\gamma)$ is also an ERA of the system, but as will be discussed in the following sections this might not be available for uncertain systems depending on the employed method. Finally, in contrast with Algorithm 1, no guarantees that the estimation is strictly non-decreasing hold.

4. Numerical examples of ERA

The nominal ERA algorithms discussed in Section 3 are applied here to two numerical examples. All the analyses are performed on a 3.6 GHz desktop PC with 16 GB RAM. Before presenting the study cases and detailed results, Table 1 summarises the computational statistics. Recall that each algorithm is iterative and each iteration features two or three Steps. Therefore, for each algorithm only the number of decision variables N_{var} and size of the Gram matrix N_{SDP} for the most demanding step are reported. In addition, the averaged processing time per iteration T_{iter} as well as the overall time T_{tot} required to determine the ERA are given.

Table 1: Computational statistics for nominal analyses

Case study	Algorithm	N_{var}	N_{SDP}	T_{iter} $[s]$	T_{tot} $[s]$
VdP (∂=4)	LF	12	142	2.5	150
VdP (∂=4)	IS - 2 Steps	27	362	4.8	88
VdP (∂=4)	IS - 3 Steps	15	362	4.4	114
VdP (∂=4)	IS - Hyb	15	362	4.5	123
SP (∂=4)	LF	120	3866	14	840
SP (∂=4)	IS - 2 Steps	246	12322	78	1872
SP (∂=4)	IS - 3 Steps	126	12322	70	1260
SP (∂=4)	IS - Hyb	246	12322	72	2742

4.1. Van der Pol oscillator

The Van der Pol (VdP) oscillator [6] is a nonlinear system with 2 states given by:

$$\begin{aligned} \dot{x}_1 &= -x_2, \\ \dot{x}_2 &= x_1 + (x_1^2 - 1)x_2. \end{aligned} \tag{11}$$

The VdP steady-state solutions are characterized by an unstable limit cycle and a stable origin. The ROA for this system is the region enclosed by its limit cycle and thus can be easily obtained from the numerical solution of the associated ordinary differential equations.

Fig. 1 shows different estimates of the ROA for this system (the aforementioned limit cycle is reported for reference and labelled *ROA*). *IS* stands for invariant sets, whereas *LF* indicates that the LF level set approach (with Algorithm 4) is adopted. For the IS approach, Algorithms 1 (*IS - 2 Steps*), 2 (*IS - 3 Steps*), and 3 (*IS - Hyb*) are tested. For the LF level set approach, the sensitivity to the selection of p is investigated and two cases are considered: $p_1 = x_1^2 + x_2^2$ (*LF-p1*) and $p_2 = 0.378x_1^2 + 0.278x_2^2 - 0.274x_1x_2$ (*LF-p2*) taken from [28]. The degree of the optimized polynomials V, V_N, R is 4 in all cases.
As a preamble, it should be noted that all the algorithms are able to provide a good approximation of the ROA of the system. In fact, VdP is often used as a

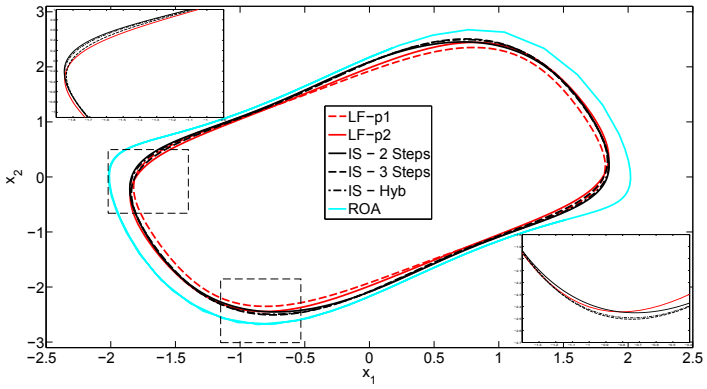

Figure 1: ERA of VdP with different approaches. $\partial(V, V_N, R) = 4$.

benchmark study for newly developed algorithms and in the same spirit was also adopted in this work. Nonetheless, a few differences among the predictions can be detected and will be commented next. Fig. 1 highlights that the invariant set approach leads to a better estimate of the ROA, and that the choice of p is important when Algorithm 4 is used. Indeed, p_1 does not specify particular directions in the phase plane, as opposed to p_2 which is *aligned* with the ROA. As a result, the estimation provided by the latter is better. This aspect is clearly displayed in this study case, and it is representative of a more general trend of the $V-s$ algorithm, whose performance is sensitive to the shape function p [28]. With regard to the invariant set approach, it can be observed that all the algorithms give in this case similar results. The small differences are better seen in the insets of Fig. 1, which help to highlight that the hybrid strategy provides overall the largest estimation of ROA among the considered approaches (note that the curve *IS - Hyb* lies close to the outermost curves in every region of the state-plane).

As for the computational statistics reported in Table 1, Algorithm 2 features a smaller T_{iter} than Algorithm 1 (bearing in mind the similarity of the results commented before). Even though the former consists of 3 steps (as opposed to Algorithm 1 which has only 2), this performance is a result of the redistribution of the computational effort driving the proposal of Algorithm 2 (also benefitting Algorithm 3). However, when looking at the overall time T_{tot} the trend is opposite, despite the fact that the two achieved estimations of the ROA are very close. This is due to the fact that the algorithms are carried out until an optimization step is unfeasible, and there is no condition preventing slow progress. Algorithm 2 performs more iterations before reaching unfeasibility, but with no tangible improvement on the estimation for this case study, and this results in a greater T_{tot}. This could be overcome by using a stopping condition based for example on one of the options discussed in Sec. 3.3 for the switching criterion sw_{cr}. Tests carried out with this rationale lead to an overall smaller time T_{tot} for Algorithm 2, too.

4.2. Controlled short-period aircraft dynamics

The second case study consists of a closed-loop nonlinear short-period (SP) model of an aircraft longitudinal dynamics [11]. It features 3 open-loop states (pitch rate z_1, angle of attack z_2, pitch angle z_3) and 2 controller states η_1, η_2.

$$\begin{aligned}
\dot{z} &= \begin{bmatrix} -3 & -1.35 & -0.56 \\ -0.91 & -0.64 & -0.02 \\ 1 & 0 & 0 \end{bmatrix} z + \begin{bmatrix} 1.35 - 0.04 z_2 \\ 0.4 \\ 1 \end{bmatrix} u \\
&+ \begin{bmatrix} 0.08 z_1 z_2 + 0.44 z_2^2 + 0.01 z_2 z_3 + 0.22 z_2^3 \\ -0.05 z_2^2 + 0.11 z_2 z_3 - 0.05 z_3^2 \\ 0 \end{bmatrix}, \\
\dot{\eta} &= \begin{bmatrix} -0.6 & 0.09 \\ 0 & 0 \end{bmatrix} \eta + \begin{bmatrix} -0.06 & -0.02 \\ -0.75 & -0.28 \end{bmatrix} y, \\
y &= \begin{bmatrix} z_1 & z_3 \end{bmatrix}^T, \quad u = \eta_1 + 2.2 \eta_2.
\end{aligned} \tag{12}$$

By defining $x = [z \quad \eta]^T$, the system is recast in the formalism of (2).

In Fig. 2 the same nomenclature as in the previous plot is adopted. The shape function p is taken as the spheroid (i.e. N is the identity matrix), and two cases differing for the degree of the polynomials are considered, (i.e. $\partial(V, V_N, R) = 2$ and 4). Since the system has more than 2 states and thus *projections* of the ERA onto particular planes have to be considered to graphically visualize the predictions. In general, the analyst will focus on the states which are supposed to experience larger perturbations during the operation of the system. In this work, the aim is to show as much information relative to the analyses as possible. Therefore, different planes for each plot will be considered, with a focus on z_1 and z_2 since the studied nonlinearities arise from their dynamics. In Fig. 2, the $z_1 - z_2$ (solid line) and $\eta_1 - \eta_2$ (dashed line) phase-planes are both depicted in each subplot.

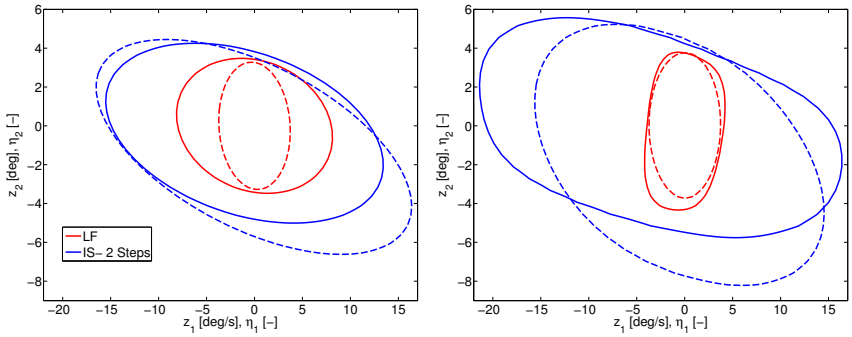

(a) $\partial(V, V_N, R) = 2$ (b) $\partial(V, V_N, R) = 4$

Figure 2: ERA of the short-period model. Different degrees of the polynomials.

The results in Fig. 2 confirm that the invariant set approach (Algorithm 1 in

this case) leads to a larger (i.e. less conservative) estimation of the ROA than the LF level set one, whose predictions obtained with an in-house implementation of the $V - s$ algorithm are in good agreement with the results presented in [11]. This is visible in all the considered planes, and for both the polynomial degrees considered.
Comparing Fig. 2(a) and Fig. 2(b) it is also apparent that if the degree is increased the obtained ERA is larger. It is worth noting that this feature is less evident for the red (LF) curves. This aspect is ascribed to the fact that, while in the invariant set algorithm the higher degree of the polynomials is fully exploited to optimize R and V_N, in the $V-s$ iteration this greater flexibility is hampered by the decisive role played by p. In these analyses, as in [11], the spheroid $p = x^T x$ was adopted and this does not exploit the directionality of the ROA observed in Fig. 2.

In general, working with larger polynomial degrees enables to improve on the estimation of the ERA. However, this inherently entails a more involved computation which, on the one hand, increases the run time, and on the other makes the SDP solution more delicate (computational aspects are detailed in Table 1). Therefore, it is interesting to perform a comparative study of the different invariant sets-based algorithms discussed in Section 3 in order to assess how they cope with this scenario. This is displayed in Fig. 3, where *IS - 3 Steps In.1* is obtained with Algorithm 2 initialized with the first iterate from Algorithm 1.

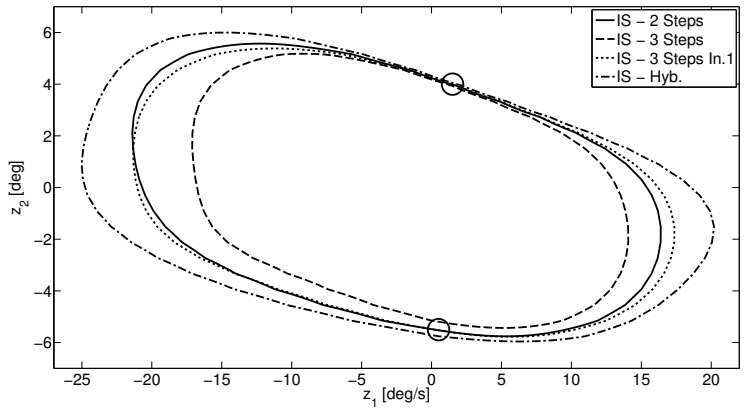

Figure 3: Sensitivity of the ERA to the iteration schemes.

The effect of the iteration scheme adopted is, as expected, more significant here than in the case of the VdP study case. In this regard, it is worth noting from Table 1 that there is an important difference in the associated computational burden. This was also commented in [11] and will be furthered in Section 5.3. Although no general conclusive remarks can be stated based on these results, it is worth discussing some trends also observed in other analyses, which considered different definitions for the multipliers and for the level set functions

degrees. The algorithms are sensitive to the initialization, especially Algorithm 2 which requires a guess for both V_N and R. When initialised with the first iterate from Algorithm 1, the use of Algorithm 2 improves the accuracy of the ROA estimation and can outperform the results of the other scheme. When the two algorithms are used in conjunction, i.e. the hybrid algorithm is employed, the estimated ERA is usually larger (as displayed in Fig. 3).

It can be appreciated from Table 1 that the reduction in T_{iter} from Algorithm 1 to Algorithm 2 is even greater for this case study. This was expected since it features a larger size in both number of states n and polynomial degree $\partial(f)$, thus the effect of lowering the SDPs dimension (which drove the design of Algorithm 2) is magnified. Algorithm 2 also features the smallest T_{tot}. Note that the high value observed for Algorithm 3 can be motivated observing that the associated ERA is markedly larger than the others and thus more iterations will be involved in its computation. This is an important aspect to keep in mind when using the metric T_{tot} to compare different algorithms.

Finally, the comparison of different ERA can enhance insight into the actual boundaries of the ROA, which is not known for the SP case. For example, from a closer inspection of Fig. 3, a dense presence of curves in some regions, marked with circles in the plot, can be identified. It can be speculated that these correspond to boundaries of the actual region of attraction of the system on the basis of an approximate overlap of the estimations given by different algorithms. These insights can be of great help since they can inform extensive refined time-marching simulations as well as provide initializations for further analyses (recall the importance of the initial guess and the possibility to exploit it in Algorithm 2 due to the required initialization of two functions).

In order to verify these inferences and quantify an upper bound on the size of the estimates, the following algorithm is proposed.

Algorithm 5.
Output: *the value of γ_f such that $\varepsilon(R,\gamma_f) \not\subset \mathcal{R}$; a set of initial conditions which do not belong to $\mathcal{R}$.*
Input: *$\partial\varepsilon(R,\gamma)$, integer N_s, and a small scalar ϵ_γ.*

1. *Simulate the nonlinear system using as initial conditions N_s random points X_0 on the boundary $\partial\varepsilon(R,\gamma)$ (extensive time-marching simulation campaign);*
2. *Define $\mathcal{F} := \left\{X_0 \in \mathbb{R}^n : \lim_{t\to\infty} \phi(t,X_0) \neq x^*\right\}$;*
3. *If $\mathcal{F} = \emptyset$, update the size $\gamma = (1+\epsilon_\gamma)\gamma$ and repeat from 1. Otherwise, $\gamma_f = \gamma$ and $\mathcal{F}$ holds a set of initial conditions which do not belong to $\mathcal{R}$.*

Algorithm 5 is applied to the level set $\varepsilon(R,\gamma)$ obtained with the hybrid iteration scheme, which gave γ=14.7. Note that in Fig. 3 the boundary of the level set is a curve because only the projection of $\varepsilon(R,\gamma)$ is displayed, but the samples X_0 in Algorithm 5 are taken on the hypersurface $\partial\varepsilon(R,\gamma)$. The algorithm, applied using $N_s = 300$ and $\epsilon_\gamma = 0.03$, returns γ_f=15.6, i.e. there is a 6% gap between the lower bound γ obtained by the hybrid scheme and the

upper bound γ_f from Algorithm 5. However, it is important to stress that Algorithm 5 gives an upper bound on the *size* of the ERA for a fixed shape R. This means that, even when the bounds are close, the ERA might still not capture accurately the region of attraction. A heuristic method to assess this consists in checking the set $\mathcal{F}$ returned by Algorithm 5. The more uniformly distributed around $\partial\varepsilon(R,\gamma)$ are the points in $\mathcal{F}$, the closer the shape of the level set is to the actual ROA. Especially when the parameter ϵ_γ is small (desirable to find a tight estimate of γ_f), the set $\mathcal{F}$ might hold only a few points. For this reason, Algorithm 5 can be run for $\gamma > \gamma_f$ in order to have a more significant collection of points.
Fig. 4 shows the results obtained applying this methodology to the SP case. Projections in two phase planes, $z_1 - z_2$ (Fig. 4(a)) and $z_2 - \eta_2$ (Fig. 4(b)), are considered. In each plot, the ERA is shown as well as cross markers corresponding to initial conditions whose trajectories do not converge to the equilibrium. Note that the markers are not confined in one area of the plane, but are distributed around distinct regions of the ERA. Specifically, the points certified to be outside of the ROA in Fig. 4(a) lie in the same regions highlighted in Fig. 3 by circle markers and discussed therein. This hints at the fact that the estimations obtained in Section 4.2 capture also the actual shape of the ROA, and not only its size as inferred from the upper bound γ_f. By increasing $\partial(V_N, R)$, an improvement on the ERA was observed along the directions where violations were not detected. Or, put it differently, where the curves in Fig. 3 were scattered.

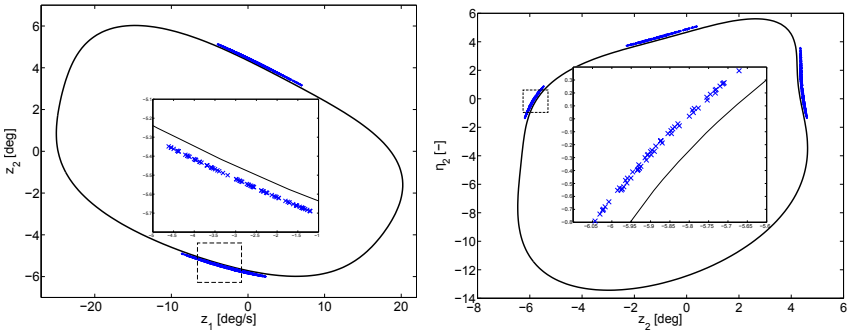

(a) Projection onto $z_1 - z_2$ plane (b) Projection onto $z_2 - \eta_2$ plane

Figure 4: Upper bounds tests on the estimated ROA.

5. Region of Attraction of systems with uncertainties

The previous sections considered the case of nominal vector fields. However, uncertainties might be present due to different sources. In fact, errors due to modeling assumptions (e.g. a local polynomial approximation of a generic vector field with associated bounded error) or parameters with uncertain values are

typically encountered in realistic engineering problems. Also, it was discussed how the use of SOS optimization often compels to limit the size of the problem (in terms of number of states n and vector field degree $2d$), therefore the dynamics might have to be simplified (e.g. higher degree terms truncation).
For these reasons, this section deals with the estimation of the Region of Attraction for systems affected by uncertainties. First, the problem is theoretically framed into the context of positively invariant sets, and an algorithm to compute robust inner Estimation of Regions of Attraction is proposed. Then, its capabilities are verified with two numerical examples and the section concludes with some important observations related to computational issues.

5.1. An algorithm for Robust Estimation of Regions of Attraction

Let us consider the system described by:

$$\dot{x} = f(x, \delta), \tag{13}$$

where $\delta \in \Delta \subset \mathbb{R}^j$ is the vector of constant unknown parameters, Δ is a known bounded set, and $f : \mathbb{R}^n \times \Delta \to \mathbb{R}^n$. It is assumed that f satisfies conditions to provide uniqueness and local existence of solutions of (13) [1] and that $f(0, \delta) = 0 \ \forall \delta \in \Delta$, i.e. the equilibrium point does not depend on the uncertainties. This latter hypothesis is largely established in the literature [13, 11, 29], although strategies to overcome this limitation have been proposed [30, 31] and could be applied here. The robust Region of Attraction (rROA) is defined as the intersection of the ROAs for all systems governed by (13):

$$\mathcal{R}_\delta := \cap_{\delta \in \Delta} \big\{ x_0 \in \mathbb{R}^n : \lim_{t \to \infty} \phi(t, x_0, \delta) = 0 \big\}, \tag{14}$$

with $\phi(t, x_0, \delta)$ denoting the solution of (13) at time t with initial condition x_0 and subject to δ.

The problem of finding a robust inner estimate of the Region Of Attraction represents an active area of research [12, 32, 33, 15], even though it has not received as much attention as the nominal case. In this work, the problem is formulated within the invariant sets approach presented in Section 4. The starting point is represented by the following result.

Theorem 2. *([9], Th. 4) Given $R : \mathbb{R}^n \to \mathbb{R}$, $V_N : \mathbb{R}^n \times \Delta \to \mathbb{R}$, $R, V_N \in \mathcal{C}^1$ and a positive scalar γ satisfying:*

$$\nabla R(x) f(x, \delta) < 0 \qquad \forall (x, \delta) \in \partial\varepsilon(R, \gamma) \times \Delta, \tag{15a}$$

$$V_N(0, \cdot) = 0 \quad \text{and} \quad V_N(x, \delta) > 0 \quad \forall (x, \delta) \in \varepsilon(R, \gamma) \backslash 0 \times \Delta, \tag{15b}$$

$$\nabla V_N(x, \delta) f(x) < 0 \qquad \forall (x, \delta) \in \varepsilon(R, \gamma) \backslash 0 \times \Delta, \tag{15c}$$

$$\varepsilon(R, \gamma) \quad \text{is compact and} \quad 0 \in \varepsilon(R, \gamma), \tag{15d}$$

then $\varepsilon(R, \gamma)$ is an invariant set of $\mathcal{R}_\delta$.

The proof follows the rationale of that for Theorem 1 (see the reference for details).

In this paper it is proposed to describe Δ as a semialgebraic set [29]:

$$\Delta = \big\{\delta \in \mathbb{R}^j : m_i(\delta) \geq 0, m_i \in \mathbb{R}[\delta], i = 1, ..., j\big\}. \tag{16}$$

This strategy is quite general and allows both time-invariant and time-varying parametric uncertainties to be taken into account, as well as norm bounded operators. Moreover, no hypotheses on how the uncertainties enter the vector field are made. This is different from previous approaches, where, for example, f is required to depend affinely on the uncertain parameters [11], or Δ must be within a polytope [12].

A useful result is recalled next.

Lemma 4. *[28] For each y satisfying $g_3(y) \leq 0$,*

$$\begin{aligned} & \{x \mid g_1(x,y) \leq 0\} \subseteq \{x \mid g_2(x,y) \leq 0\}, \\ \text{iff} \quad & \{(x,y) \mid g_1(x,y) \leq 0, g_3(y) \leq 0\} \subseteq \{(x,y) \mid g_2(x,y) \leq 0\}. \end{aligned} \tag{17}$$

It is stressed that the last set-containment can be easily enforced with Lemma 2.

Based on these preliminaries, the following Lemma allowing to study robust ERA within the framework of invariant sets is stated.

Lemma 5. *Given $R \in \mathbb{R}[x]$, $V_N \in \mathbb{R}[x,\delta]$ with $V_N(0,\cdot) = 0$, and a positive scalar γ, if there exist $s_1, s_2, s_{0i}, s_{1i}, s_{2i} \in \Sigma[x,\delta]$ and $s_0 \in \mathbb{R}[x,\delta]$ such that:*

$$-\nabla R f - s_0(\gamma - R) - \Gamma_{0j} \in \Sigma[x,\delta], \tag{18a}$$

$$V_N - s_1(\gamma - R) - \Gamma_{1j} \in \Sigma[x,\delta], \tag{18b}$$

$$-\nabla V_N f - s_2(\gamma - R) - \Gamma_{2j} \in \Sigma[x,\delta], \tag{18c}$$

$$\text{with} \quad \Gamma_{\#j} = s_{\#1}m_1 + ...s_{\#i}m_i + ... + s_{\#j}m_j, \quad \# = 0,1,2 \tag{18d}$$

then the conditions of Theorem 2 are satisfied and $\varepsilon(R,\gamma) \subseteq \mathcal{R}_\delta$.

Proof. The proof of (18a)⇒(15a) is given here. By virtue of the uncertainty description in (16), condition (15a) can be stated as

$$\begin{aligned} & \text{For each } \delta \text{ satisfying } m_i(\delta) \geq 0, \text{ (for } i = 1, ..., j) \\ & \big\{x : \gamma - R(x) = 0\big\} \subseteq \big\{x : -\nabla R f(x,\delta) \geq 0\big\}. \end{aligned} \tag{19}$$

For Lemma 4, this holds if and only if

$$\big\{(x,\delta) : \gamma - R(x) = 0, m_i(\delta) \geq 0, i = 1, ..., j\big\} \subseteq \big\{(x,\delta) : -\nabla R f(x,\delta) \geq 0\big\}. \tag{20}$$

This set containment constraint is in the form of (6). Indeed, it is enough to take $h = \gamma - R(x)$, $f_i = m_i$ and $f_0 = -\nabla R f(x,\delta)$. By applying the generalized S-procedure (Lemma 2) it is obtained the SOS constraint (18a), which hence provides a sufficient condition for (15a) to hold. A similar rationale applies to the other constraints in the Lemma. □

This Lemma compounds results previously commented in the article, and provides a novel recipe for the determination of robustly invariant sets. The corresponding program to enlarge the provable rERA is:

Program 2.

$$\begin{aligned} &\max_{s_1,s_2,s_{0i},s_{1i},s_{2i}\in\Sigma[x,\delta];\ s_0,V_N\in\mathbb{R}[x,\delta];\ R\in\mathbb{R}[x]} \gamma \\ &\text{subject to conditions (18a-18b-18c).} \end{aligned} \tag{21}$$

Program 2 leads again to bilinearities and, to tackle this, adaptations of Algorithms 1, 2, and 3 can be employed. As an example, the extension of Algorithm 2 is reported next. Notice that, despite the apparent similarities with the latter, Algorithm 6 allow to extend the invariant set framework to the uncertainty case in a formal manner by addition of the terms $\Gamma_{\#j}$. Their role and other distinctive features of this approach are commented later.

Algorithm 6. *(IS_R - 3 Steps)*
Output: *the level set $\varepsilon(R,\gamma)$ (parameter-independent inner estimate of the rROA).*
Input: *polynomials R^0, V_N^0 satisfying (18) for some γ.*

Step A6-1 : optimize the multipliers for fixed level sets shapes

$$\begin{aligned} &\max_{s_1,s_2,s_{0i},s_{1i},s_{2i}\in\Sigma[x,\delta];\ s_0\in\mathbb{R}[x,\delta]} \gamma \\ &-\nabla R^0 f - s_0(\gamma - R^0) \quad - \Gamma_{0j} \in \Sigma[x,\delta] \\ &V_N^0 - s_1(\gamma - R^0) - \Gamma_{1j} \qquad \in \Sigma[x,\delta] \\ &-\nabla V_N^0 f - s_2(\gamma - R^0) - \Gamma_{2j} \in \Sigma[x,\delta] \end{aligned}$$

set $\bar{s}_\# \leftarrow s_\#, \# = 0,1,2$

Step A6-2 : optimize V_N

$$\begin{aligned} &\max_{V_N\in\mathbb{R}[x,\delta]} \gamma \\ &-\nabla R^0 f - \bar{s}_0(\gamma - R^0) - \bar{\Gamma}_{0j} \ \in \Sigma[x,\delta] \\ &V_N - \bar{s}_1(\gamma - R^0) - \bar{\Gamma}_{1j} \qquad \in \Sigma[x,\delta] \\ &-\nabla V_N f - \bar{s}_2(\gamma - R^0) - \bar{\Gamma}_{2j} \in \Sigma[x,\delta] \end{aligned}$$

set $\bar{V}_N \leftarrow V_N, \bar{\gamma} \leftarrow \gamma$

Step A6-3 : optimize R

$$\begin{aligned} &\max_{s_3\in\Sigma[x,\delta];\ R\in\mathbb{R}[x]} \gamma \\ &-\nabla R f - \bar{s}_0(\gamma - R) - \bar{\Gamma}_{0j} \quad \in \Sigma[x,\delta] \\ &\bar{V}_N - \bar{s}_1(\gamma - R) - \bar{\Gamma}_{1j} \qquad \in \Sigma[x,\delta] \\ &-\nabla \bar{V}_N f - \bar{s}_2(\gamma - R) - \bar{\Gamma}_{2j} \in \Sigma[x,\delta] \\ &(\gamma - R) - s_3(\gamma_2 - R^0) \qquad \in \Sigma[x,\delta] \end{aligned}$$

set $R^0 \leftarrow R, V_N^0 \leftarrow \bar{V}_N$ and go to Step A6-1

where $\Gamma_{\#j}$ is defined in (18d) and $\bar{\Gamma}_{\#j} = \bar{s}_{\#1}m_1 + ...\bar{s}_{\#i}m_i + ... + \bar{s}_{\#j}m_j$. In addition to the options discussed previously for the nominal case, the initialization of R and V_N can be done with the corresponding functions obtained

with the ERA calculation. The independent variables of the optimization now include the states of the system x and the uncertain parameters δ. The polynomial multipliers s can thus potentially be function of both x and δ (as reported in Algorithm 6), but in practice there is a trade-off between computational time and accuracy. One of the advantages of this formulation is that the level set function is $R = R(x)$ (i.e. uncertain parameter-independent), whilst V_N is parameter dependent, i.e. $V_N(x, \delta)$. On the one hand, this is a less conservative approach than the one represented by parameter-independent LF level sets. On the other, the fact that $\varepsilon(R, \gamma)$ is parameter-independent avoids the computation of the intersection of the parameterised estimates, resulting in a more accurate and easier to visualise outcome. This favorable twofold behaviour is the result of using two distinct functions, R and V_N, which allows for greater flexibility in the optimization.

The description of the set in (16) entails the definition of the polynomials m_i, which depend on the type of uncertainties featuring the system. This work will focus on parametric uncertainties, and thus possible definitions will be discussed for this case. Let us denote with $\underline{\delta}_i$ and $\overline{\delta}_i$ the minimum and maximum allowed values for each uncertain parameter δ_i respectively. Then, at each parameter a polynomial m_i can be associated as follows:

$$\begin{aligned} &m_i(\delta_i) = -(\delta_i - \underline{\delta}_i)(\delta_i - \overline{\delta}_i), \\ &\delta \in \Delta \iff m_i(\delta_i) \geq 0, \\ &\delta = [\delta_1 ... \delta_i ... \delta_j]^T. \end{aligned} \tag{22}$$

Recalling the definition of $\Gamma_{\#j}$ in (18d), it is worth noting that for each employed m_i there are three multipliers s_{0i}, s_{1i}, s_{2i} (one for each constraint). Therefore, as the number of uncertain parameters increases, so does the size of the associated optimization problem. However, an alternative solution is to define a single polynomial m_c:

$$\begin{aligned} &m_c(\delta) = -\sum_{i=1}^{j}(\delta_i - \underline{\delta}_i)(\delta_i - \overline{\delta}_i) = \sum_{i=1}^{j} m_i(\delta_i), \\ &\delta \in \Delta \Longrightarrow m_c(\delta) \geq 0, \end{aligned} \tag{23}$$

which specializes (18d) to $\Gamma_{\#1} = s_{\#c} m_c$.
This definition gives only a sufficient condition (as opposed to the one in (22) which is also necessary), because there are values of $\delta \notin \Delta$ for which the inequality $m_c(\delta) \geq 0$ is satisfied. Therefore, the obtained rERA is valid for a larger range of uncertainties. However, the adoption of m_c has the advantage of adding only 3 multipliers s_{0c}, s_{1c}, s_{2c} regardless of the number of uncertainties.

5.2. Uncertain Van der Pol oscillator

In [11] the VdP with an uncertain scalar parameter $\delta_1 \in [-1, 1]$ was considered. Its dynamic is:

$$\begin{aligned} \dot{x}_1 &= -x_2(1 + 0.2\delta_1), \\ \dot{x}_2 &= x_1 + (x_1^2 - 1)x_2. \end{aligned} \tag{24}$$

The estimation of the ROA was performed in [11] via parameter-independent LF enforcing the constraints used in the V-s iteration on both vertices of the uncertainty range (in full generality, the method prescribes to do this on each vertex of the uncertain polytope).
Fig. 5 shows the rERA obtained applying the extensions of Algorithm 1 (IS_R - *2 Steps*), Algorithm 2 (IS_R - *3 Steps*), and the hybrid approach (IS_R - *Hyb*) to the scenario with uncertainties. The cases with $\partial(V, V_N, R) = 4$ (Fig. 5(a)) and $\partial(V, V_N, R) = 6$ (Fig. 5(b)) are plotted. $V_N(x, \delta_1)$ is built from monomials in x and δ_1 up to degree $\partial(V_N)$, with the property that $V_N(0, \cdot) = 0$. All the algorithms are initialised with the functions V_N and R from nominal analyses. The predictions from [11] are displayed labelled as *LF*, along with the unstable limit cycle of the system corresponding to eight values of δ_1 across its range ($ROA(\delta)$).

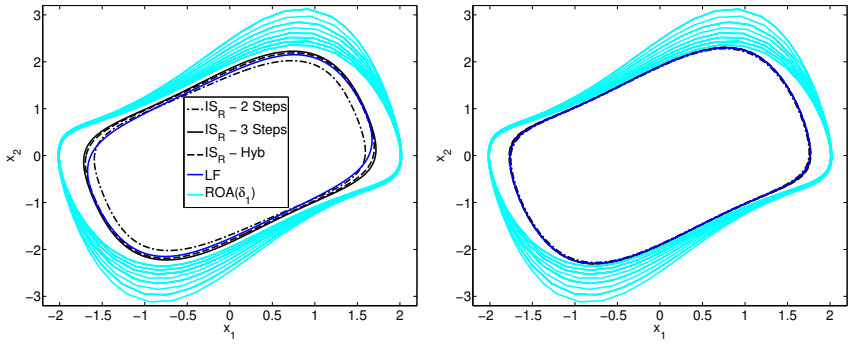

(a) $\partial(V, V_N, R) = 4$ (b) $\partial(V, V_N, R) = 6$

Figure 5: Robust estimates of the region of attraction for the uncertain VdP.

In both cases the rERA obtained with the invariant set approaches are larger than the level sets from [11], although in Fig. 5(b) they are very close. Moreover, the algorithm IS_R - *3 Steps* outperforms in these cases the other two IS_R algorithms. Table 2 provides the computational aspects.

Table 2: Computational statistics for rERA of VdP $\partial = 4$

Algorithm	N_{var}	N_{SDP}	T_{iter} $[s]$	T_{tot} $[s]$
LF	30	392	3.5	175
IS - 2 Steps	54	1200	17.5	105
IS - 3 Steps	24	1200	13.5	270
IS - Hyb	54	1200	15	217

5.3. Uncertain controlled short-period aircraft dynamics

The uncertain short-period was studied in [11, 34]. Compared to the nominal plant (12), two parametric uncertainties δ_1 and δ_2 affect now the open loop dynamics:

$$\begin{aligned}\dot{z} = &\begin{bmatrix} -3 & -1.35 & -0.56 \\ -0.91 & -0.64 & -0.02 \\ 1 & 0 & 0 \end{bmatrix} z + \begin{bmatrix} 1.35 - 0.04 z_2 \\ 0.4 \\ 1 \end{bmatrix} u \\ &+ \begin{bmatrix} (1+\delta_1)(0.08 z_1 z_2 + 0.44 z_2^2 + 0.01 z_2 z_3 + 0.22 z_2^3) \\ (1+\delta_2)(-0.05 z_2^2 + 0.11 z_2 z_3 - 0.05 z_3^2) \\ 0 \end{bmatrix}, \\ &\delta_1, \delta_2 \in [-0.1, 0.1].\end{aligned} \tag{25}$$

In [11, 34] the adopted algorithms were based on: (i) a suboptimal strategy to avoid enforcing the $V - s$ iteration at each vertex of the polytope [11]; and (ii) a branch-and-bound refinement of the suboptimal algorithm consisting in partitioning the uncertainty set and determining a different parameter-independent LF for each cell [34]. In both cases, the rERA was expressed in the form of $\varepsilon(p, \beta)$ because a unique LF V certifying the ROA over the entire uncertainty set was not computed by the algorithms.

The plot in Fig. 6 shows the analyses using $\partial(R, V_N) = 2$ (the nomenclature of Fig. 5(a) applies). The largest estimate available in the published literature, taken from [34] and obtained with quartic LFs employing the suboptimal (branch-and-bound refined) algorithm, corresponds to $\beta = 11.1$ and $p = x^T x$ and is reported in here for comparison. Projections of the rERA onto the $z_1 - z_2$ plane (Fig. 6(a)) and $z_1 - z_3$ plane (Fig. 6(b)) are depicted. The results showcase that the three proposed rERA algorithms based on invariant sets are close to each other and outperform the estimation given with the LF level set approach (which was obtained with a higher degree for the LF). The analyses in Fig. 6 were obtained describing the uncertainty set with a single polynomial $m_c(\delta_1, \delta_2)$ following the definition in (23).

Similar to the nominal case, an upper bound on the rERA of Fig. 6 is evaluated making use of an extension of Algorithm 5. Since now the system is subject to uncertainties, the evaluation of N_δ random samples of the uncertainty vector δ is performed first and, for each of them, Algorithm 5 is applied. Similar investigations to the one discussed at the end of Section 4.2 can be applied to assess in detail the accuracy of the estimation. The Algorithm 5 is used here to determine the smallest value of γ_f such that $\varepsilon(R, \gamma_f) \notin \mathcal{R}_\delta$. Tests are conducted using $N_\delta = 100$, $N_s = 300$, and $\epsilon_\gamma = 0.03$. The results are visualised in Fig. 7 by plotting the projections of $\varepsilon(R, \gamma_f)$ (giving an upper bound UB) and $\varepsilon(R, \gamma)$ (giving a lower bound LB) onto the same planes used in Fig. 6.

Finally, in Table 3 are reported the computational statistics for the algorithms employed to determine Fig. 7. Note that in [34] there is no reference to computational time or size of the problem. However, in [11] a smaller estimation (i.e. without branch-and-bound refinement) was achieved in approximately 2300

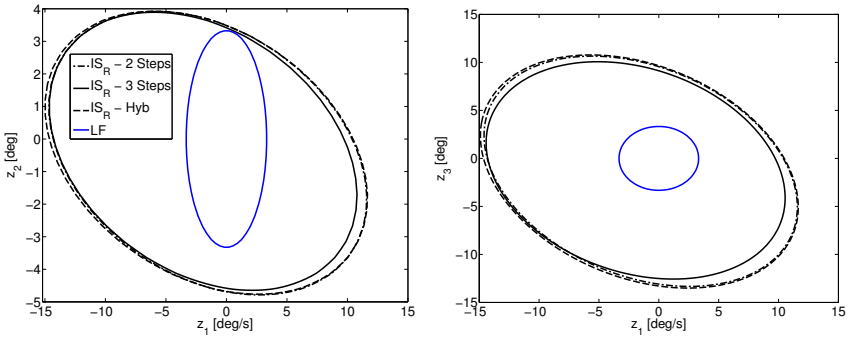

(a) Projection onto $z_1 - z_2$ plane (b) Projection onto $z_1 - z_3$ plane

Figure 6: Robust estimates of the region of attraction for the uncertain SP.

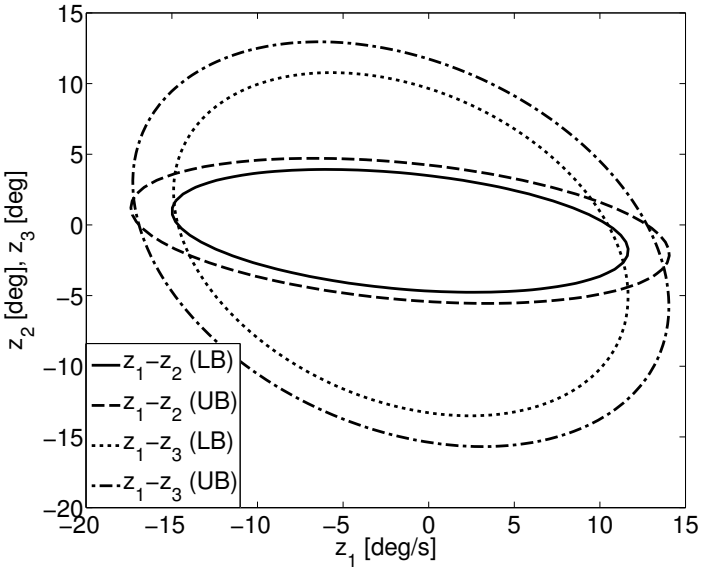

Figure 7: Upper and lower bounds of the rERA.

seconds (and this is taken as lower bound on the total processing time of algorithm *LF*).

5.4. Computational issues related to SOS optimization

It is well-known in the community that the usefulness of SOS in optimization and control studies is partially mitigated by the so-called *scalability*, i.e. the significant growth in simulation time and corresponding decrease in computational efficiency, as the size of the analysed system increases. Although no conclusive statistics can be given, well established teams [11, 35] have concurred in setting

Table 3: Computational statistics for robust analyses - SP $\partial = 2$

Algorithm	N_{var}	N_{SDP}	T_{iter} $[s]$	T_{tot} $[s]$
LF	-	-	-	> 2300
IS - 2 Steps	744	41772	220	2420
IS - 3 Steps	714	41772	210	1890
IS - Hyb	744	41772	203	2770

a limit on the problems that can be solved currently via a direct SOS based analysis in approximately $n \cong 6$ number of variables and $\partial(g) \cong 4$ polynomials degree.

The short-period example from Section 5.3 features 5 states, nonlinearities up to degree 3 and also includes 2 uncertainties, thus it represents a challenging case study for the state of practice of ROA analysis tools. In the article, algorithmic strategies, such as the adoption of different iteration schemes and approximated polynomial descriptions of semialgebraic sets, have been proposed in order to provide with alternative ways to solve the optimization problem so that difficulties in the convergence with one strategy do not hamper the estimation of the ROA. A concrete example of the sensitivity of the rERA to the size of the SOS problem is shown here with regard to the adoption of different descriptions for the uncertainty set.
The analyses in Fig. 6 were obtained with a single polynomial m_c and it is thus interesting to investigate which differences arise when the necessary and sufficient condition in (22) is employed. Fig. 8 shows the comparison, based on the 2 Steps algorithm, between the case of one single polynomial (m_c) and the case when one polynomial per each uncertainty is used (m_i, $i = 1, 2$). The result from the level set approach (LF) is plotted for reference and again two projections are used (in the $z_1 - z_2$ and $z_2 - \eta_2$ planes).
It can be noted that, although the definition of the uncertainty set with m_c is in principle more conservative, it provides in this case a larger estimate of the robust ROA. Indeed resorting to a stronger but cheaper description (23) might have the benefit of relaxing the underlying optimization, and thus provide a more tractable numerical problem. It is for this reason that the alternative option proposed in this work (consisting of only one term and thus only one multiplier) can represent an advantage when dealing with systems of medium-large size (to be interpreted in the context of SOS problems).

The research community is actively working on rigorous improvements to the well recognised issue of computational efficiency in the application of SOS techniques. For example, in [35] a method to decompose nonlinear dynamical systems into lower order ones and then compute the stability certificates on the latter is proposed. This method, suitable for systems which have a modular structure, can be further expedited if sparsity is imposed on the polynomials calculated for each subsystem. Different ways of exploiting sparsity are reviewed

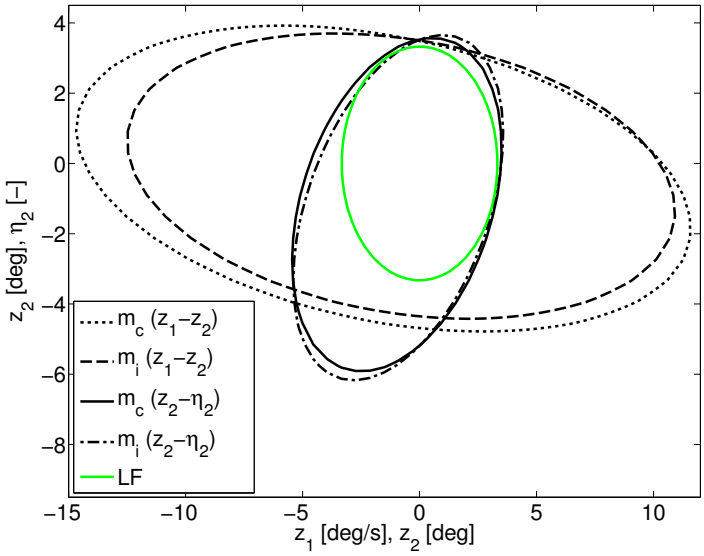

Figure 8: Comparison of results with different descriptions of the uncertainties.

in [36], where a survey on recent advances in the SOS technique is presented. One idea, originally proposed in [37], is to relax the requirement that the Gram matrix Q is semidefinite with stronger but cheaper conditions. Namely, diagonally dominant and scaled diagonally dominant matrices Q are sought so that $g = z^T Q z$ still implies that the polynomial g is non-negative. This has the benefit that the optimization underpinning the determination of Q is a linear and a second order cone program respectively, in both cases more tractable that an SDP.

These references (and those cited therein) show the potential for efficient advanced numerical tools which can make the SOS programs presented in this article more amenable for higher order systems.

6. Conclusions

This article considers the problem of estimating the region of attraction of nominal and uncertain nonlinear systems described by polynomial vector fields. A recently proposed formulation based on invariant (but not contractive) level sets is adopted as the theoretical foundation to propose computationally efficient calculation algorithms for nominal ROA.

The above is then extended to the study of uncertain nonlinear systems, which is the main contribution of the article. The uncertainties are described as a semi-algebraic set and new conditions are derived which allow the study of robust region of attractions. This approach can handle various types of uncertainties and does not make restrictive hypotheses on the dependence of the vector field on them.

The article comments also on well-known computational issues associated with the usage of Sum Of Squares relaxations, and possible heuristic solutions to ameliorate them are discussed. An iteration scheme to tackle the bilinearities arising in the corresponding programs is proposed, and the advantages of jointly use different iterative algorithms in order to overcome infeasibility or slow progress is demonstrated via two example systems.
For the presented study cases, the invariant sets algorithms outperform the ones based on Lyapunov functions level sets (well established in the community and considered here for benchmarking). The advantage in adopting the invariant set approach is more pronounced when the size of the analysed system is increased, and the same holds for the adoption of the specific iterative schemes proposed in this article. Finally, upper bounds on the estimated ROA evaluated by means of extensive time-marching simulation campaigns confirm accuracy in capturing both the size and the shape of the ROA.
Future works can, on the one hand, apply recent results in the SOS community in order to make the analysis of higher order system with proposed framework more computationally efficient. On the other hand, the idea of adopting an hybrid search for the estimation of ROA can be furthered by studying possible switching criteria and quantifying their performance.

Acknowledgements

This work has received funding from the Horizon 2020 research and innovation programme under grant agreement No 636307, project FLEXOP.
The authors would like to thank Prof. Pete Seiler for helpful discussions about ROA and SOS.

References

[1] H. K. Khalil, Nonlinear systems, Prentice Hall, 1996.

[2] R. Genesio, M. Tartaglia, A. Vicino, On the estimation of asymptotic stability regions: State of the art and new proposals, IEEE Transactions on Automatic Control 30 (8) (1985) 747–755.

[3] G. Valmorbida, S. Tarbouriech, G. Garcia, Region of attraction estimates for polynomial systems, in: 48th IEEE Conference on Decision and Control (CDC), 2009.

[4] G. Chesi, Domain of Attraction: Analysis and Control via SOS Programming, Springer, 2011.

[5] A. Chakraborty, P. Seiler, G. Balas, Susceptibility of F/A-18 Flight Controllers to the Falling-Leaf Mode: Nonlinear Analysis, J. of Guidance, Control and Dynamics 34 (1) (2011) 73–85.

[6] W. Tan, A. Packard, Stability Region Analysis Using Polynomial and Composite Polynomial Lyapunov Functions and Sum-of-Squares Programming, IEEE Transactions on Automatic Control 53 (2) (2008) 565–571.

[7] D. Henrion, M. Korda, Convex Computation of the Region of Attraction of Polynomial Control Systems, IEEE Transactions on Automatic Control 59 (2) (2014) 297–312.

[8] A. Iannelli, P. Seiler, A. Marcos, Estimating the Region of Attraction of uncertain systems with Integral Quadratic Constraints, 57th IEEE Conference on Decision and Control (CDC), 2018.

[9] G. Valmorbida, J. Anderson, Region of attraction estimation using invariant sets and rational Lyapunov functions, Automatica 75 (2017) 37 – 45.

[10] D. Han, A. El-Guindy, M. Althoff, Estimating the Domain of Attraction Based on the Invariance Principle, in: 55th IEEE Conference on Decision and Control (CDC), 2016.

[11] U. Topcu, A. Packard, Local Stability Analysis for Uncertain Nonlinear Systems, IEEE Transactions on Automatic Control 54 (5) (2009) 1042–1047.

[12] U. Topcu, A. K. Packard, P. Seiler, G. J. Balas, Robust Region-of-Attraction Estimation, IEEE Transactions on Automatic Control 55 (1) (2010) 137–142.

[13] G. Chesi, Estimating the domain of attraction for uncertain polynomial systems, Automatica 40 (2004) 1981 – 1986.

[14] A. Trofino, T. J. m. Dezuo, LMI stability conditions for uncertain rational nonlinear systems, International Journal of Robust and Nonlinear Control 24 (18) (2013) 3124 3169.

[15] P. Polcz, T. Peni, G. Szederkenyi, Improved algorithm for computing the domain of attraction of rational nonlinear systems, European Journal of Control, (2017).

[16] J. Anderson, A. Papachristodoulou, Advances in computational Lyapunov analysis using sum-of-squares programming, Discrete and Continuous Dynamical Systems - Series B 20 (8) (2015) 2361–2381.

[17] A. Iannelli, A. Marcos, M. Lowenberg, Algorithms for the estimation of the region of attraction with positively invariant sets, 7th International Conference on Systems and Control (ICSC), 2018.

[18] A. Iannelli, A. Marcos, M. Lowenberg, Estimating the region of attraction of uncertain systems with invariant sets, 9th IFAC Symposium on Robust Control Design (ROCOND), 2018.

[19] P. Parrilo, Structured Semidefinite Programs and Semialgebraic Geometry. Methods in Robustness and Optimization, Ph.D. thesis, California Institute of Technology (2000).

[20] S. Boyd, L. El Ghaoui, E. Feron, V. Balakrishnan, Linear Matrix Inequalities in System and Control Theory, Society for Industrial and Applied Mathematics (SIAM), 1994.

[21] G. J. Balas, A. K. Packard, P. Seiler, U. Topcu, Robustness analysis of nonlinear systems, http://www.aem.umn.edu/ AerospaceControl/.

[22] J. F. Sturm, Using SeDuMi 1.02, A Matlab toolbox for optimization over symmetric cones, Optimization Methods and Software 11 (1-4) (1999) 625–653.

[23] J. Bochnak, M. Coste, M.-F. Roy, Real Algebraic Geometry, Springer, 1998.

[24] P. Seiler, G. Balas, Quasiconvex Sum-of-Squares Programming, in: 49th IEEE Conference on Decision and Control (CDC), 2010.

[25] M. Kocvara, M. Stingl, PENBMI Users Guide (Version 2.1) (2006).

[26] Z. Michalewicz, D. Fogel, How ro Solve It: Modern Heuristics, 2nd Edition, Springer-Verlag, 2004.

[27] P. P. Menon, J. Kim, D. G. Bates, I. Postethwhite, Clearance of Nonlinear Flight Control Laws Using Hybrid Evolutionary Optimization, IEEE Transactions on Evolutionary Computation 10 (6) (2006) 689–699.

[28] W. Tan, Nonlinear Control Analysis and Synthesis using Sum-of-Squares Programming, Ph.D. thesis, University of California Berkeley (2006).

[29] J. Anderson, A. Papachristodoulou, Robust nonlinear stability and performance analysis of an F/A-18 aircraft model using sum of squares programming, International Journal of Robust and Nonlinear Control 23 (10) (2013) 1099 1114.

[30] E. M. Aylward, P. A. Parrilo, J. E. Slotine, Stability and robustness analysis of nonlinear systems via contraction metrics and SOS programming, Automatica 44 (8) (2008) 2163 – 2170.

[31] A. Iannelli, P. Seiler, A. Marcos, An equilibrium-independent region of attraction formulation for systems with uncertainty-dependent equilibria, 57th IEEE Conference on Decision and Control (CDC), 2018.

[32] G. Chesi, Rational Lyapunov functions for estimating and controlling the robust domain of attraction, Automatica 49 (2013) 1051 – 1057.

[33] A. Zecevic, D. Siljak, Estimating the region of attraction for large-scale systems with uncertainties, Automatica 46 (2009) 445 – 451.

[34] U. Topcu, A. Packard, P. Seiler, G. Balas, Local stability analysis for uncertain nonlinear systems using a branch-and-bound algorithm, American Control Conference, 2008.

[35] J. Anderson, A. Papachristodoulou, A Decomposition Technique for Nonlinear Dynamical System Analysis, IEEE Transactions on Automatic Control 57 (6) (2012) 1516–1521.

[36] A. A. Ahmadi, G. Hall, A. Papachristodoulou, J. Saunderson, Y. Zheng, Improving Efficiency and Scalability of Sum of Squares Optimization: Recent Advances and Limitations, in: 56th IEEE Conference on Decision and Control (CDC), 2017.

[37] A. A. Ahmadi, A. Majumdar, DSOS and SDSOS Optimization: More Tractable Alternatives to Sum of Squares and Semidefinite Optimization, ArXiv e-prints, 2017,arXiv:1706.02586.